II International Conference on Particle-based Methods – Fundamentals and Applications
PARTICLES 2011
E. Oñate and D.R.J. Owen (Eds)

NUMERICAL SIMULATIONS OF SAND BEHAVIOUR USING DEM WITH TWO DIFFERENT DESCRIPTIONS OF GRAIN ROUGHNESS

J. KOZICKI AND J. TEJCHMAN

Civil and Environmental Engineering Department
Gdańsk University of Technology
Gdańsk, Poland
e-mail: jkozicki@pg.gda.pl, tejchmk@pg.gda.pl

Key words: DEM, Dissipation, Energy, Grain Roughness, Sand, Triaxial Test

Abstract. A quasi-static homogeneous drained triaxial compression test on cohesionless sand under constant lateral pressure was simulated using a three-dimensional DEM model. Grain roughness was modelled by two different approaches: first with contact moments applied to rigid spheres and second with clusters of rigid spheres imitating irregular particle shapes. The effect of the grain roughness (shape) on shear strength, dilatancy, energy and dissipation was analyzed using both models. Numerical results were directly compared with experimental results on Karlsruhe sand.

1 INTRODUCTION

Granular materials consist of grains in contact and of surrounding voids, which change their arrangement depending on environmental factors and initial density. Their micromechanical and fabric behaviour is inherently discontinuous, heterogeneous and non-linear. To describe their behaviour, two main approaches are used: continuum and discrete ones. The first ones perform simulations at the global scale using the finite element method on the basis of e.g. elasto-plastic and hypoplastic constitutive models enhanced by a characteristic length of micro-structure to describe strain localization. In turn, the latter ones perform simulations at the grain scale, i.e. each grain is modelled individually. Their advantages are that they directly model micro-structure and can be used to comprehensively study the mechanism of the initiation, growth and formation of shear zones at the micro-level which strongly affect macro-properties of granular matter. The disadvantages are: high computational cost, inability to model grain shape accurately, difficulty to validate it experimentally and inertial effects and damping effects lose their meaning in quasi-static problems. However, they become more and more popular nowadays for modelling granular materials due to an increasing speed of computers and a connection possibility to the finite element method.

Many experimental and numerical studies revealed that irregularly shaped grains strongly affect the quasi-static mechanical behavior of granular materials. To resemble the real grain shape (roughness), two main approaches are usually used: 1) contact moments between rigid spheres or disks [1-6]) or clusters of combined discrete elements that form irregularly-shaped grains [7-11].

In this paper, numerical studies of quasi-static homogeneous axisymmetric triaxial compression tests were carried out to determine the macroscopic behaviour of a sand

specimen composed of discrete elements. The three-dimensional discrete model YADE developed at University of Grenoble was used [3]. The particle breakage has not been considered. Discrete simulation results were quantitatively compared with the corresponding experimental data from drained axisymmetric triaxial compression tests performed by Wu [12] at Karlsruhe University with real sand. The intention of our studies was to calculate the effect of the grain roughness (shape) using these two above mentioned methods on the shear strength, dilatancy, energy and dissipation of real sand (so-called Karlsruhe sand), which had the same initial void ratio, mean grain diameter and grain distribution. Such a direct comparison of the effect of grain roughness using 2 different approaches has not been performed yet. A special attention was paid to the energy transformation in sand and its elastic and dissipative characteristics, playing an important role in the granular matter behaviour. The energy and dissipation results were compared with the similar ones during two-dimensional simulations of biaxial compression with round particles performed by Kruyt and Rothenburg [13] and by Bi et al. [14].

2 DISCRETE ELEMENT METHOD

The discrete element method (DEM) is widely used to model a range of processes across many industries. To simulate the behaviour of sand, a three-dimensional spherical discrete model YADE was developed at University of Grenoble [3] by taking advantage of the so-called soft-particle approach (i.e. the model allows for particle deformation which is modeled as an overlap of particles). A dynamic behaviour of the discrete system is solved numerically using a force-displacement Lagrangian approach and tracks the positions, velocities, and accelerations of each particle individually. It uses an explicit finite difference algorithm assuming that velocities and accelerations are constant in each time step. To calculate forces acting in particle-particle or particle-wall contacts, a particle interaction model is assumed in which the forces are typically subdivided into normal and tangential components. The total forces acting on each particle are summed. Next, the problem is reduced to the integration of Newton's equations of motion for both translational and rotational degrees of freedom. As the results, the accelerations of each particle are obtained. The time step is incremented and accelerations are integrated over time to determine updated particle velocities and positions. To maintain the numerical stability of the method and to obtain a quick convergence to a quasi-static state of equilibrium of the assembly of particles, damping forces have to be introduced [15]. To increase the rolling resistance, contact moments between spheres (caused by the normal force) were introduced [3]. Figure 1 shows the mechanical response of contact models.

The following five main local material parameters are needed for discrete simulations: E_c, (modulus of elasticity of the grain contact), υ_c Poisson's ratio of the grain contact), μ (inter-particle friction angle), β (rolling stiffness coefficient) and η (plastic rolling coefficient) using spheres with contact moments (E_c, υ_c and μ without contact moments). In addition, the particle radius R, particle density ρ and damping parameters α are required. The material parameters were calibrated with corresponding axisymmetric triaxial laboratory test results on Karlsruhe sand by Wu [12]. The index properties of Karlsruhe sand are: mean grain diameter d_{50}=0.50 mm, grain size among 0.08 mm and 1.8 mm, uniformity coefficient U=2, maximum specific weight γ_d^{max}=17.4 kN/m^3, minimum void ratio e_{min}=0.53, minimum specific weight γ_d^{min}=14.6 kN/m^3

and maximum void ratio e_{max}=0.84. The following discrete material parameters for rigid spheres with contact moments were assumed for discrete studies: E_c=0.30 GPa, ν_c=0.3, μ=30^o, η=0.2, β=0.1, ρ=2.6 kNs^2/m^4, α=0.08 and d_{50}=5.0 mm.

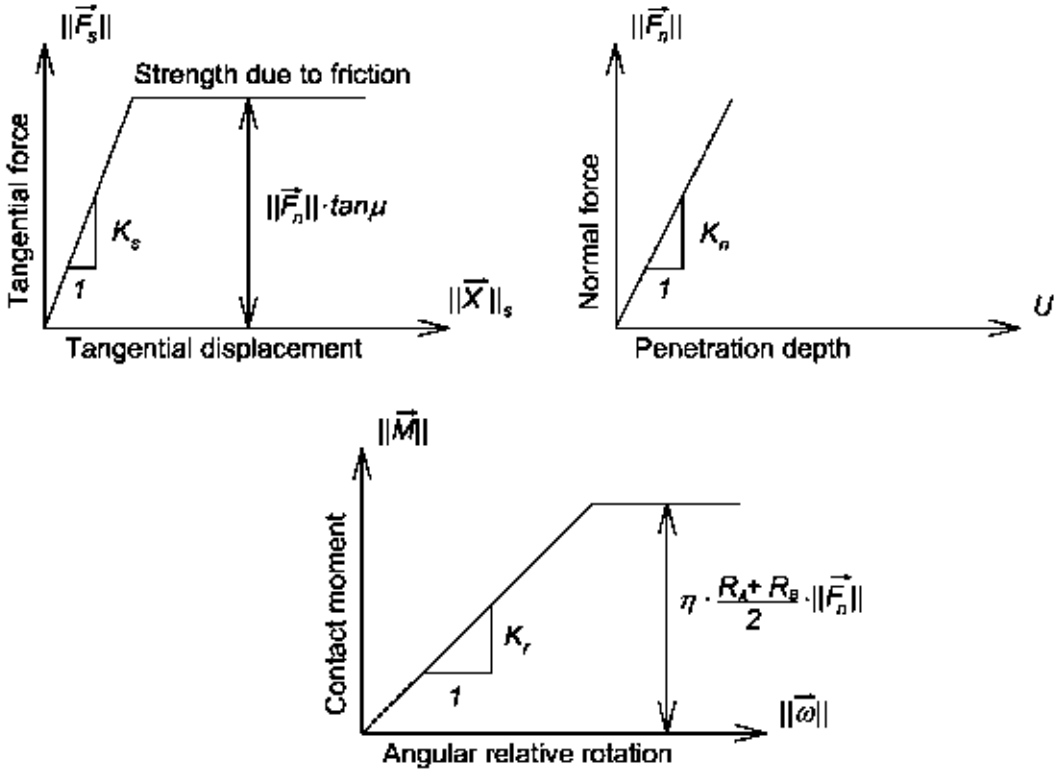

Figure 1: Mechanical response of contact models: a) tangential contact model, b) normal contact model and c) rolling contact model [3]

In numerical simulations, a cubic sand specimen of 10×10×10 cm^3 was used. A simplified linear grain distribution curve was used for Karlsruhe sand (grain range among 2 mm and 8 mm). In order to save the computation time, remaining discrete simulations showing the capabilities of DEM were carried out with d_{50}=5 mm instead of d_{50}=0.5 mm. The test was modelled using confining smooth rigid wall elements (without inducing shear localization). The top and bottom boundaries moved vertically as loading platens under strain-controlled conditions to simulate the confining pressure p. To ensure the test was conducted under quasi-static conditions, the loading speed was slow enough. The initial configuration of the sand specimen was isotropic. Each assembly was prepared by first dropping the particles into the container under a gravitational field with the friction coefficient between particles set to zero. Gravity was varied to obtain a desired initial density caused by grain overlapping (thus, it was possible to exactly reproduce the experimental initial sand volumetric weight). The assembly was then allowed to settle to a state where the kinetic energy was negligible, before it is compressed under an initial confining pressure. The isotropic assembly was then subjected to boundary driven triaxial compression.

Figure 2 presents the 12 different clusters of spheres used in discrete calculations. In the case of the cluster of 2 spheres without the overlap (shape '*f*'), 26'300 clusters were used composed of 52'600 spheres. In turn, 28'250 clusters were used with 197'750 spheres to model simple ellipsoids (shape '*i*') and 14'500 clusters were used with 594'500 spheres to model disks (shape '*l*'). In the case of 3D calculations with spheres using contact moments, 6'600 spheres were used.

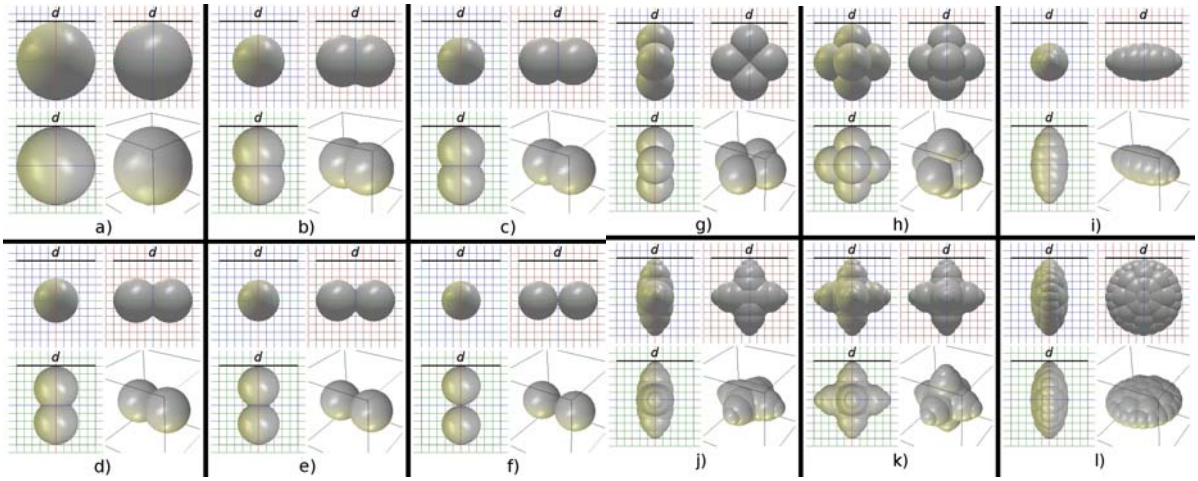

Figure 2: Different symmetric grain shapes created by clusters of hard spheres used for discrete simulations (*d* - grain diameter)

3 DISCRETE RESULTS OF TRIAXIAL TEST

3.1 Effect of grain roughness (shape) on strength and volume changes

Figure 3 shows the calculated evolution of the vertical normal stress and overall void ratio versus vertical normal strain for different clusters of spheres of Fig.2 (without contact moments) during triaxial compression with initially dense sand (e_o=0.53, d_{50}=5 mm) under confining pressure of p=200 kPa. Similarly as in the real experiment (Fig.3), the initially dense specimens exhibits initially elasticity, hardening (connected to contractancy and dilatancy), reaches a peak at about of ε_l=3%, gradually softens and dilates reaching at large vertical strain of 25-30% the same value of the vertical normal stress with the granular specimen deforming at constant volume, i.e. a critical state is always reached. Thus, the particle shape is not essential for the global critical internal friction angle (except of the case with spheres). The both mobilized strength and dilatancy increase with increasing grain roughness (rolling resistance) combined with an increase of the sphere number. Thus, the irregularly shaped particles provide obviously higher internal friction angles and have less tendency to rotate than perfect circular particles. The global maximum mobilized internal friction angle increases from ϕ_{max}=28° (spheres) up to ϕ_{max}=48.9° (disks), respectively (Fig.3). In turn, the global residual internal friction angle increases from ϕ_{cr}=15° (spheres '*a*' of Fig.2) up to ϕ_{cr}=31° (disks '*l*' of Fig.2), respectively (Fig.3). The dilatancy angle ψ raises from ψ=5°

(spheres) up to ψ=30^o (disks), respectively. The elastic modulus is also similar independently of the grain roughness. The granular system shows small fluctuations in the residual phase.

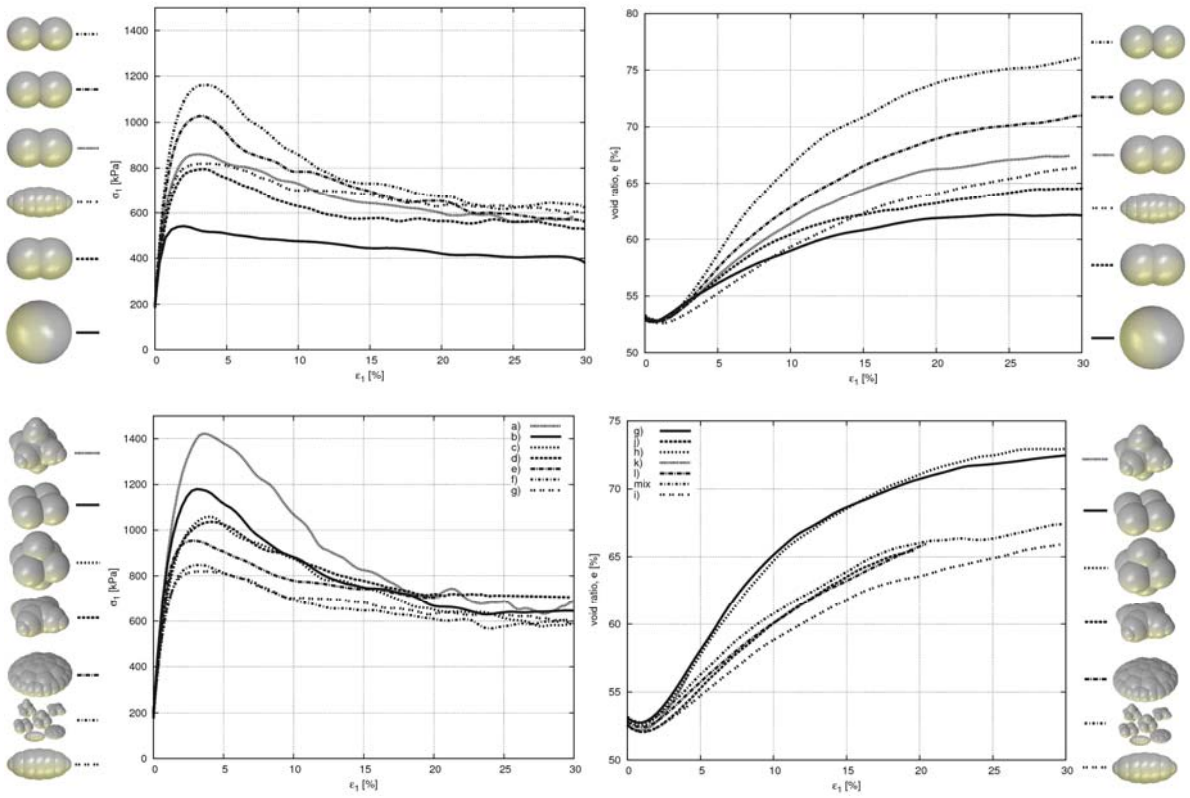

FIGURE 3: Effect of particle roughness (without contact moments) on vertical normal stress σ_1 versus vertical normal strain ε_1 (A) and volumetric strain ε_v versus vertical normal strain ε_1 (B) during homogeneous triaxial compression test for different grain shapes of Fig.4 (e_o=0.53, p=200 kPa, d_{50}=5 mm)

Figure 4 shows a direct comparison between different granular clusters composed of 2 ellipsoids, 2 spheres and 6 spheres without contact moments, pure spheres with contact moments and experiments (Wu 1992). All curves are qualitatively the same. The global maximum internal friction angle is 42.5° at ε_1=5% (spheres with contact moments) and 41°-(clusters) ε_1=3%. In turn, the global residual internal friction angle is 32.5° (spheres with contact moments) and 31° (clusters). As compared to the results with spheres with contact moments, the best agreement with experiments provides clusters of 6 spheres. Note that it is possible to calibrate more accurately a discrete model with each grain shape of Fig.2 with respect to laboratory tests.

3.2 Effect of grain roughness (shape) on energy and dissipation

In the granular system there exist 3 main energies: the elastic energy, kinetic energy and energy dissipation. In addition, numerical dissipation also exists. The elastic internal energy stored at contacts between grains E_e is done by elastic contact tangential forces on tangential

elastic displacements U_t, contact normal forces on penetration depths U and elastic contact moments on elastic rotations ω (when contact moments are considered). In general, the elastic internal energy is (N- contact number). The kinetic energy E_c of grains is caused by their translation and rotation. Due to quasi-static conditions, the effect of E_c is negligible (less than 1%). The energy plastic dissipation D_p is due to plastic (shear) tangential forces and plastic (shear) moments during slip (sliding) and rotation (see Fig.1). In addition, numerical dissipation D_n takes place during translation and rotation. The total accumulated energy $E=E_e+E_c+D_p+D_n$ is equal to the external boundary work W done on the assembly by 6 external forces on displacements of 6 rigid external walls.

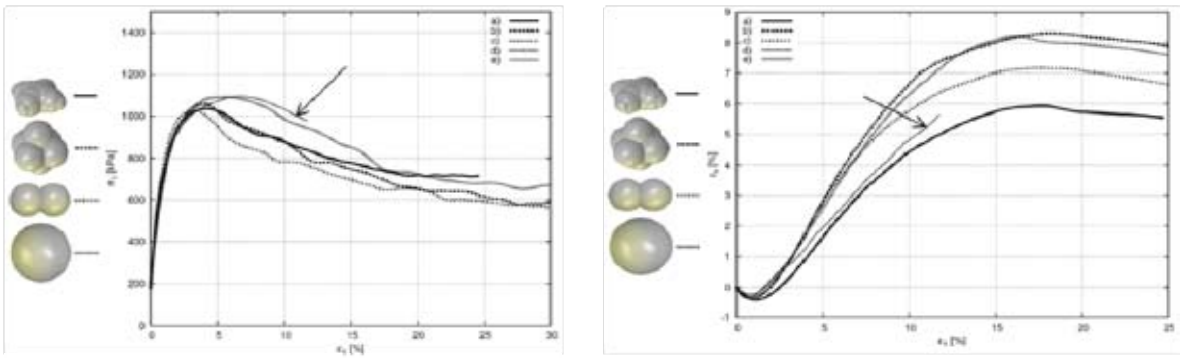

A) B)

FIGURE 4: Effect of some clusters of spheres of Fig.2 without contact moments and single spheres with contact moments on vertical normal stress σ_1 versus vertical normal strain ε_1 (A) and volumetric strain ε_v versus vertical normal strain ε_1 (B) compared to experiments ($\rightarrow$) during homogeneous triaxial compression test (e_o=0.53, p=200 kPa, d_{50}=5 mm)

Figure 5 shows the calculated effect of the grain roughness on the total accumulated energy E, elastic internally stored energy at contacts E_e, plastic dissipation D_p and numerical damping D_n (Eq.8) in initially dense sand (e_o=0.53, p=200 kPa, d_{50}=5.0 mm). Compared were the systems composed of spheres with contacts moments and systems of clusters of 2 spheres and 6 spheres without contact moments (Fig.2). In turn, the evolution of the external energy rate δE, elastic internal energy rate δE_e and plastic dissipation rate δD_p is demonstrated in Fig.6. Finally, Figure 7 demonstrates the evolution of the kinetic energy of the systems.

There exists a roughly linear relationship between the total energy and plastic damping against the vertical normal strain (Fig.5). The plastic dissipation during frictional sliding is equal at the strain of ε_1=3% (corresponding to the maximum vertical stress) to 50% of the total energy (irregularly-shaped grains). At the residual state of ε_1=30%, it is already equal to 88% (irregularly-shaped grains) of the total energy. The numerical damping is equal always to 6% of the total energy. The evolution of three components of the elastic internal energy is similar to the evolution of the shear strength (the maximum value is at ε_1=5%) (Fig.3). At the beginning of deformation at ε_1<1% (when the specimen is in the elastic range), the total energy is almost fully converted into the elastic energy. The change of the elastic internal work is initially positive. It rapidly approaches zero and a small negative value at about ε_1=5% (Fig.6) and afterwards slightly increases approaching an asymptote at zero. Beyond

strains of ε_1=5%, almost the entire input work is dissipated due to plastic deformation and numerical damping (the external energy rate and dissipation rate are equal $\delta W \cong \delta D$).

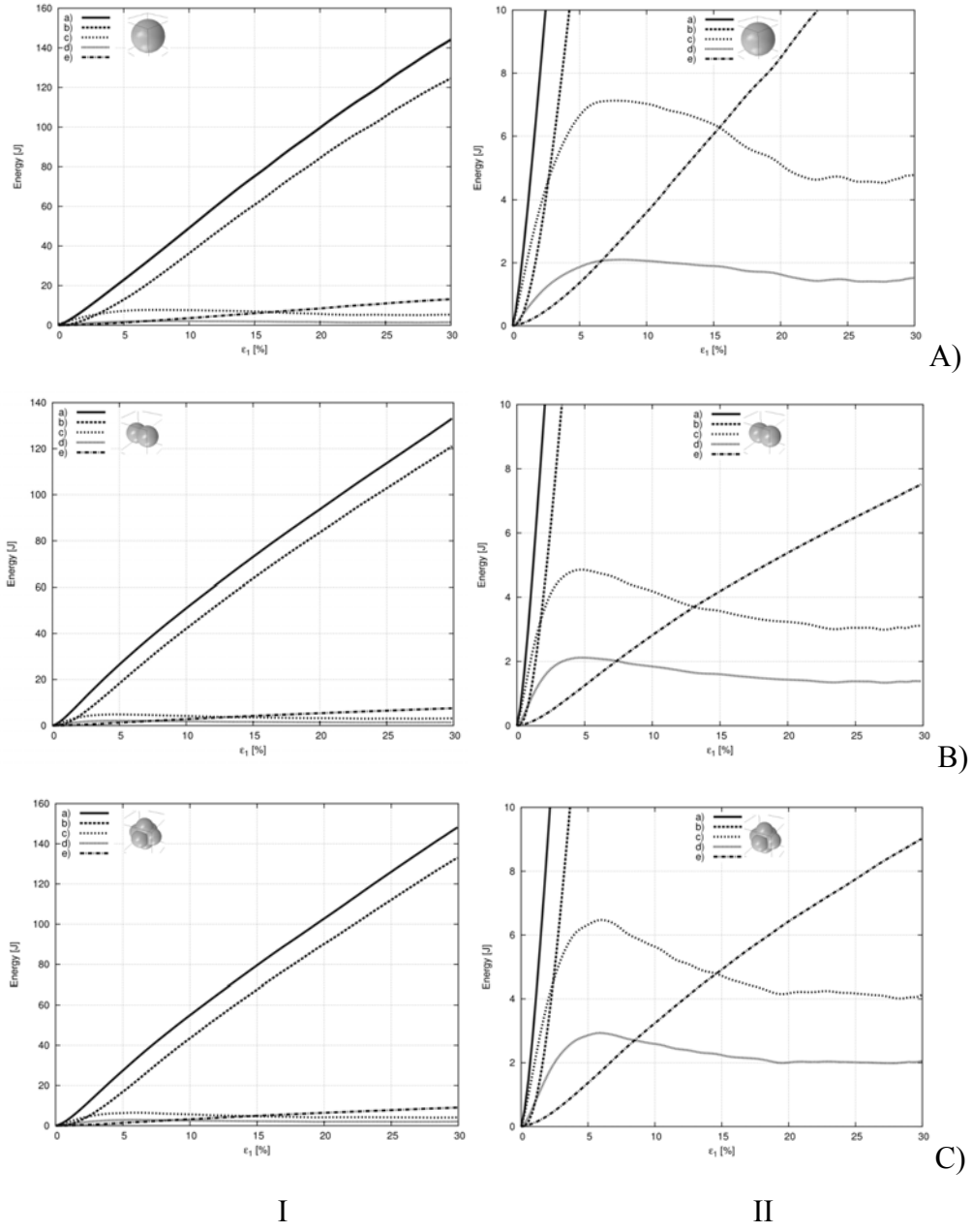

Figure 5: Calculated evolution of: a) total energy W, b) plastic dissipation D_p, c) elastic work in normal direction E_c^n, d) elastic work in tangential direction E_c^s, e) numerical non-viscous damping D_n during homogeneous triaxial compression test for: A) single spheres with contact moments, B) clusters of 2 spheres, C) clusters of 6 spheres (e_o=0.53, p=200 kPa, d_{50}=5 mm) (I) wide view, II) zoom)

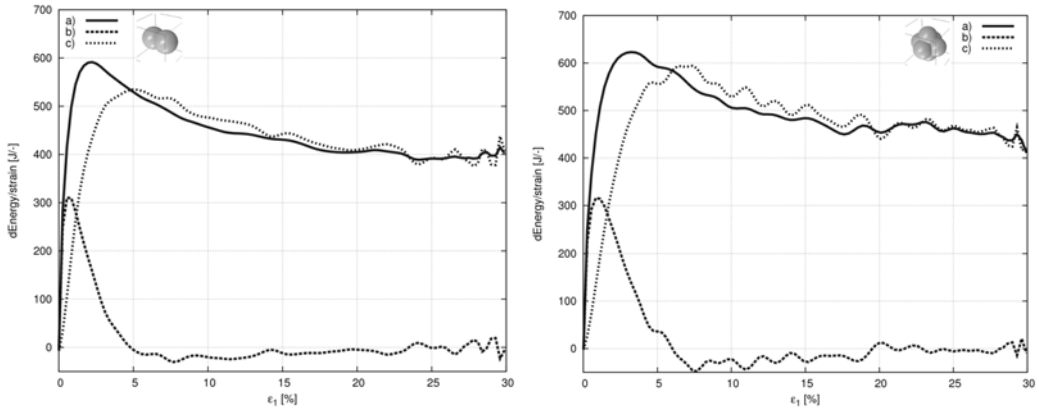

Figure 6: Calculated evolution of: a) external energy rate δW, b) elastic internal work rate δE_c and c) plastic energy dissipation rate δD during homogeneous triaxial compression test: A) clusters of 2 spheres, B) clusters of 6 spheres (e_o=0.53, p=200 kPa, d_{50}=5 mm)

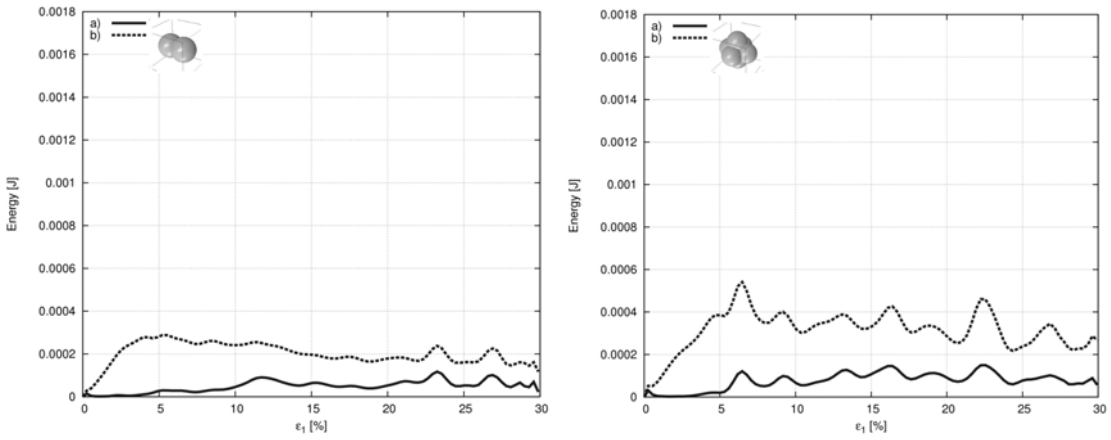

Figure 7: Calculated evolution of kinetic energy E_c during homogeneous triaxial compression test: A) clusters of 2 spheres, B) clusters of 6 spheres (e_o=0.53, p=200 kPa, d_{50}=5 mm), a) translational kinetic energy, b) rotational kinetic energy

The elastic internal work is 80% at ε_1=1%, 40% at ε_1=3% and 5% at ε_1=30% (irregularly-shaped grains) of the total energy, respectively. The residual elastic internal work is performed by contact normal forces in 70%, by contact tangential forces in 20% and by contact moments in 10% in the case of single spheres with contact moments, and by contact normal forces in 70% and contact tangential forces in 30% with irregularly-shaped grains. Thus, the largest internal work is performed by contact normal forces and the smallest one by contact moments. The elastic energy ratio is the same at the residual state.

The evolution curves in Figs.5 are qualitatively similar to those demonstrated by Bi et al. [14]. In turn, the evolution curves in Fig.6 are slightly different in the initial phase than those

shown by Kruyt and Rothenburg [13], which were calculated using periodic boundary conditions. The calculated energy quantities are different than in analyses by Bi et al. [14] using the software of PFC2D (where e.g. the calculated elastic energy was significantly higher: 90% (at ε_l=3%) and 20% (at ε_l=5%) of the total energy.

The kinetic energy is very small due to the quasi-static loading of the granular system (Fig.7). A release of the elastic energy drives grains to move. At the elastic stage, the rotational kinetic energy is close to zero. After it increases and slightly decreases. At the residual phase, the kinetic energy shows fluctuations which correspond to the evolution of the elastic energy and damping rate.

4 CONCLUSIONS

The numerical simulations of a homogeneous triaxial compression test show that a discrete model is capable to reproduce the most important macroscopic properties of cohesionless granular materials without it being necessary to describe the granular structure perfectly. Comparing the numerical simulations with the experimental triaxial tests conducted for different initial void ratios and confining pressures shows that the model is able to realistically predict the experimental results for cohesionless sand. The following detailed conclusions can be also drawn:

- The model is capable of closely reproducing the behaviour of cohesionless soils in the elastic, contraction, and dilatancy phase and at the critical state. At large strains, the granular specimen reaches always a critical state independently of its initial density. The higher the confining pressure, the smaller are both the global friction and dilatancy.
- The sand grain roughness can be modelled by means of spheres with contact moments or irregularly-shaped grains. The calculations with spheres are significantly faster, but those with irregularly-shaped grains are more realistic.
- The largest internal work is performed by contact normal force and the smallest one by contact moments.
- At the elastic stage, the boundary external work is mainly converted into elastic energy. At the residual state, the almost total external boundary work is dissipated by plastic deformation.
- The kinetic energy is very small due to quasi-static loading. The translational kinetic energy is higher than the rotational one.

Our research will be continued. The discrete simulations will be carried with sand during biaxial compression out by taking into account shear localization. The local phenomena occurring in a shear zone (such as buckling of granular columns, vortices, force chain cycles, periodic alternating dilatancy and contractancy) will be carefully studied.

Acknowledgment

Scientific work has been carried out as a part of the Project: “Innovative resources and effective methods of safety improvement and durability of buildings and transport infrastructure in the sustainable development” financed by the European Union

REFERENCES

[1] Iwashita K. and Oda M. Rolling resistance at contacts in simulation of shear band development by DEM. *ASCE J Eng Mech.* (1998) **124**(3):285–92.

[2] Jiang, M.J., Yu, H.-S. and Harris, D. A novel discrete model for granular material incorporating rolling resistance. *Computers and Geotechnics* (2005) **32**:340-357.

[3] Kozicki, J. and Donze, F.V. A new open-source software developed for numerical simulations using discrete modelling methods. *Computer Methods in Applied Mechanics and Engineering* (2008) **197**:4429-4443.

[4] Belheine, N., Plassiard, J.P., Donze, F. V., Darve, F. and Seridi, A. Numerical simulations of drained triaxial test using 3D discrete element modeling. *Computers and Geotechnics* (2009) **36** (1-2):320-331.

[5] Mohamed, A. and Gutierrez, M. Comprehensive study of the effects of rolling resistance on the stress-strain and strain localization behavior of granular materials. *Granular Matter* (2010) **12** (5):527-541.

[6] Widulinski, L., Tejchman, J., Kozicki, J. and Leśniewska, D. Discrete simulations of shear zone patterning in sand in earth pressure problems of a retaining wall. *Int. J. Solids and Structures* (2011) **48** (7-8):1191-1209.

[7] Ng, T.-T. Particle shape effect on macro- and micro-behaviors of monodisperse ellipsoids. *Int. J. Numer. Anal. Meth. Geomech.* (2009) **33**, 511-52.

[8] Salot, Ch., Gotteland, P. and Villard, P. Influence of relative density on granular materials behaviour: DEM simulations of triaxial tests. *Granular Metter* (2009) **11** (4):221-236.

[9] Ferellec, J.-F. and McDowell, G.R. A method to model realistic particle shape and inertia in DEM. *Granular Matter* (2010) **12**:459-467.

[10] Maeda, K., Sakai, H., Kondo, A., Yamaguchi, T., Fukuma, M. and Nukudani, E. Stress-chain based micromechanics of sand with grain shape effect. *Granular Matter* (2010) **12:**499-505.

[11] Matsushima, T. and Chang, C.S. Quantitative evolution of the effect of irregularly shaped particles in sheared granular assemblies. *Granular Matter* (2011) **13:**269-276, 2011.

[12] Wu, W. Hypoplastizität als mathematisches Modell zum mechanischen Verhalten granularer Stoffe. *Heft 129, Institute for Soil- and Rock-Mechanics, University of Karlsruhe*, 1992.

[13] Kruyt, N.P. and Rothenburg, L. Shear strength, dilatancy, energy and dissipation in quasi-static deformation of granular materials. *Journal of Statistical Mechanics* (2006) P07021: 1-10.

[14] Bi, Z., Sun, Q., Jin, F. ·and Zhang, M. Numerical study on energy transformation in granular matter under biaxial compression. *Granular Matter* (2011) **13**:503–510.

[15] Cundall, P.A. and Strack, O.D L. The distinct numerical model for granular assemblies *Geotechnique* (1979) **29**:47-65.